17th World Conference on Earthquake Engineering, 17WCEE
Sendai, Japan - September 13th to 18th 2020

AN EFFECTIVE VIBRATION CONTROL SYSTEM FOR SUPER-SLENDER BUILDINGS

Atsushi NISHIMOTO[(1)], Katsuhide MURAKAMI[(2)]

[(1)] *Staff, Structural Design Section, Engineering Department, NIKKEN SEKKEI LTD, nishimoto.atsushi@nikken.jp*
[(2)] *Director, Structural Design Section, Engineering Department, NIKKEN SEKKEI LTD, murakamik@nikken.jp*

Abstract

In super-slender buildings, axial deformation governs column design rather than bending or shear deformation. This deformation is caused by axial load fluctuation. In this paper, the author proposes a solution in the form of a vibration control system using a core shaft frame with vertical viscous dampers at the base and TMDs at the top floor. By controlling the vibration modes, dampers perform more effectively and fully impart supplementary damping. To test the performance, we designed and built a 14-story super-slender steel moment resisting frame (MRF) with core truss frames, with a slenderness ratio of 9.6 (including the rooftop structure) and the natural period is approximately 2.3s. A dynamic analysis was also undertaken considering design ground motions with a constant velocity response spectrum of 100 cm/s in the long period range. Unlike general MRF systems, the proposed system suppresses top deformation effectively. The performance variation of the vertical viscous dampers and TMDs to seismic response was also studied, revealing that the performance variation has little influence. It should be emphasized that the influence of damping performance variations is small, and that modal control is highly effective for mitigating the deformation for the following reasons; (1) Buildings with sufficient damping have small absolute fluctuations of damping, even if the damping performance varies, (2) Damping mechanisms with heavy mass like TMDs tend to resemble mid-story isolation systems and tend to be less-sensitive against various disturbances.

Keywords: Damping; Vibration-mode control; TMD; Oil damper; Viscous damper

1. Introduction

Seismic damping systems are often chosen over seismic isolation for multi-story buildings in small sites. They are useful when the building deformation needs to be reduced but there is no room for required clearance for a seismic isolation system. Typically, dampers are installed diagonally on every floor as shown in Fig. 1. Sometimes they are installed across multiple stories in order to concentrate deformations and make the s more effective at resisting shear deformation [1].

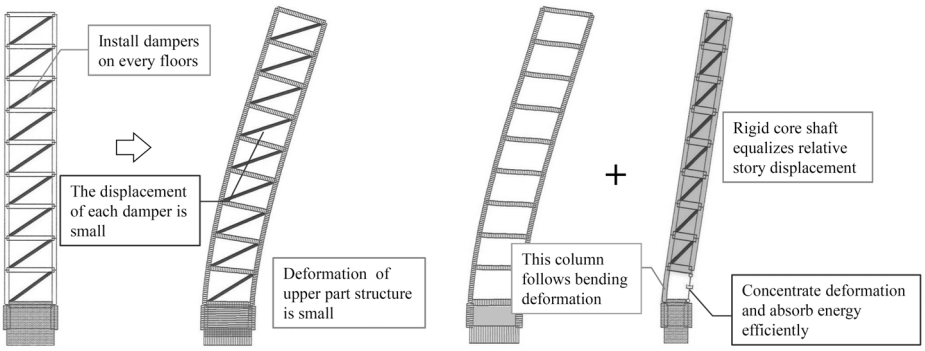

(a) General super-slender building frame (b) Proposed super-slender building frame

Fig.1 – Frame concept

However, for a structure with a high aspect ratio, bending deformation caused by axial load fluctuations often governs the total deformation. This makes the diagonal dampers less effective, and the ones installed at

upper floors likely to provide little benefit. The diagonal layout also restricts architectural planning, especially for a building with such a small footprint. For example, the ground floor is the most effective place to control the building deformation, but this significantly restricts planning of the entrance. For ease of floor planning, the diagonal dampers should be laid out at the perimeter of the building (although this has undesired visual impacts on the building façade). This can degrade the commercial value of the architecture. This paper proposes a super-slender steel MRF system with vibration controls that can reduce horizontal deformation by effective damping dynamic energy, while minimizing the impact on the architectural planning. The deformation control system consists of the following:

1. Core shaft frame

The core shaft frames around the elevator shafts are stiffened with bracing and integrated with vertical viscous dampers at ground level (as shown in Fig. 2) in order to resist bending deformation. With these, the frames can average the story drifts, so that the building vibration is characterized by lower modes.

2. Vertical viscous damper

The interior columns of the aforementioned core shaft frames are integrated with vertical viscous dampers at the ground level only. This system leads to energy dissipation through deformation equalization effects of the core shaft frame, where the horizontal displacement is translated to vertical displacements and concentrated.

3. Tuned Mass Damper (TMD)

Two TMDs are installed on the rooftop. They are laid out along the short direction at each end in order to mitigate the dominant shaking in the short direction and the accompanying torsion of the building. They are tuned to the 1st mode which, in this case, is predominant during seismic loading.

2. Structural Design Introduction

We applied the proposed system to a 14-story super-slender steel moment resisting frame (MRF) with a core truss conforming to the Japanese Building Code. The structural concept is shown in Fig. 2. It has eight vertical viscous dampers at ground level and two TMDs on the roof top. The TMDs are designed to move only in the short direction.

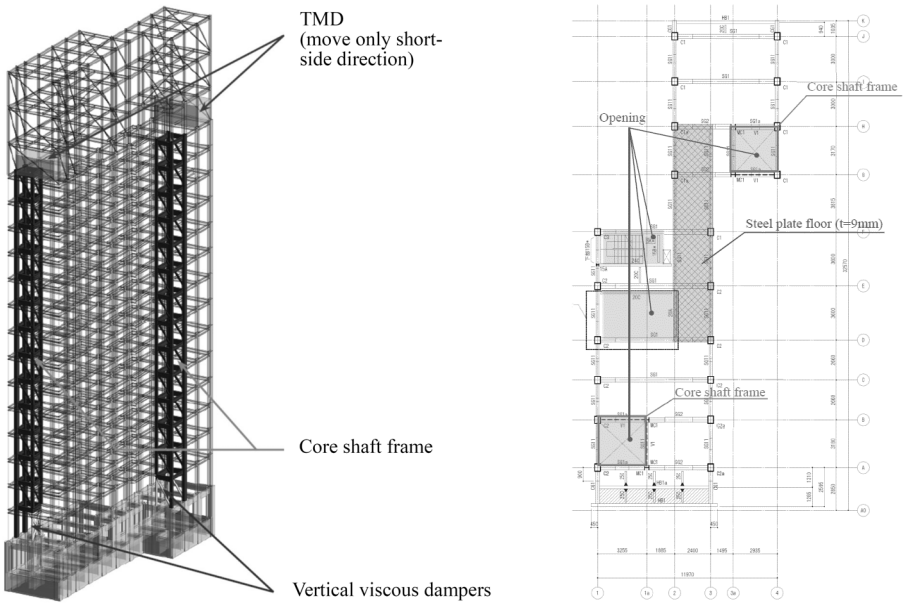

(a) Structural system (b) Standard floor plan

Fig.2 – Structural frame concept diagram (Cont.)

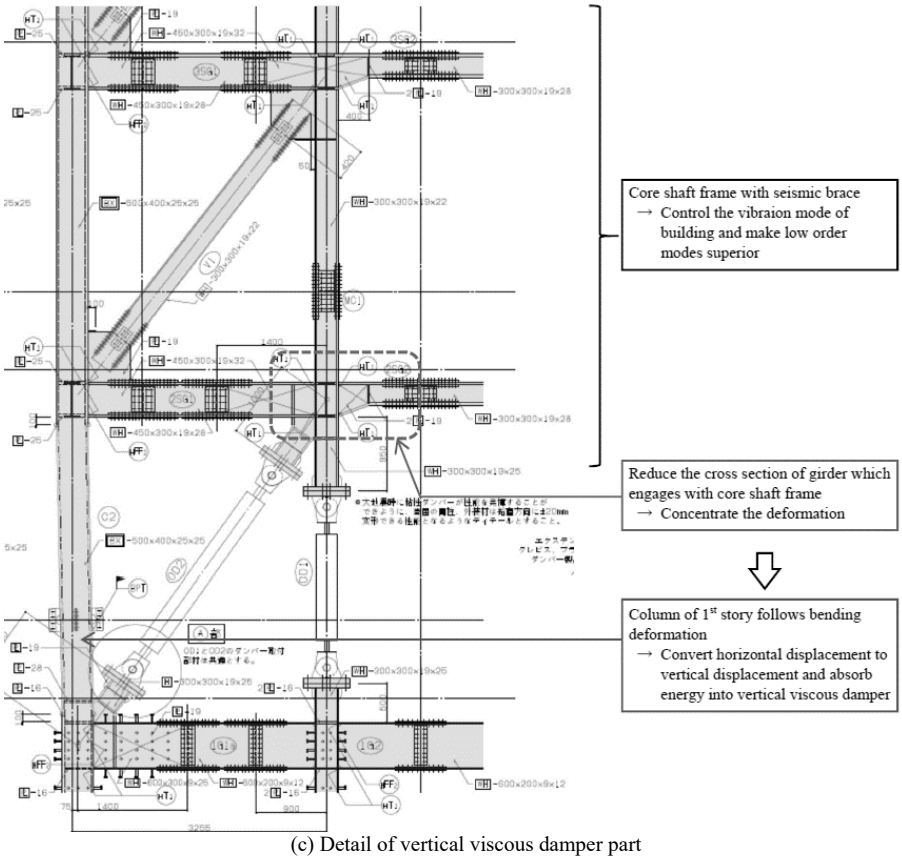

(c) Detail of vertical viscous damper part

Fig.2 – Structural frame concept diagram

The aspect ratio is 9.6 (considering also the height of the rooftop structure). The 1st and 2nd Eigen periods are 2.22 and 1.86 seconds, respectively. Both modes show building sway in the short direction coupled with torsion. The modal periods and mode shapes are summarized in Table 1 along with the higher frequency modes.

3. Static and Modal Characteristics

We applied the proposed system to a 14-story super-slender steel moment resisting frame (MRF) with a core truss conforming to the Japanese Building Code. The structural concept is shown in Fig. 2. It has

3.1 The effectiveness of core shaft frame

This section discusses the effects of the core shaft frames from the viewpoint of its modal characteristics. The contribution of the core shaft frame (as shown in Fig. 3(a)) to the seismic response of each mode is evaluated by comparing to a case without them (as shown in Fig. 3(b)). The participation factors of 1st to 4th mode are summarised in Table 2. Participation factor is calculated as shown in Equation (1).

$$PF_i = |EF_i| / \sum_{i=0}^{10} |EF_i| \qquad (1)$$

PF_i is the participation factor of the i-th order mode. EF_i is excitation factor of the i-th order mode. As can be seen from Table 1, the X (short-side) direction 1st mode and Torsion (R_Z) direction 1st mode are coupled. Then, X direction 1st mode and R_Z 1st mode are defined total 1st mode. It has been confirmed that about 95% of the participating mass ratio is considered with 10 modes.

Table 1 – Eigen mode and period

	1st mode	2nd mode	3rd mode
X	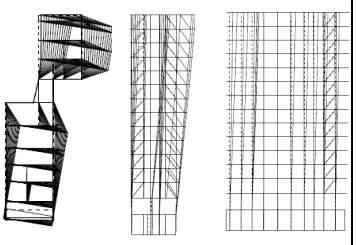	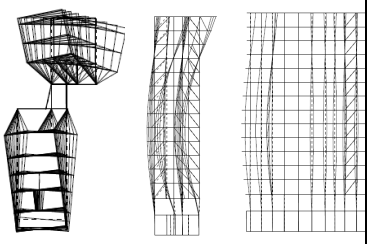	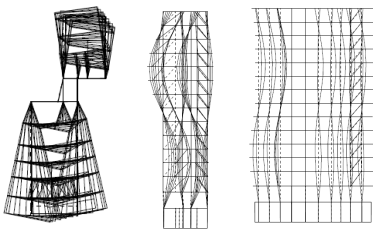
	1.86 [s]	0.52 [s]	0.31 [s]
Y	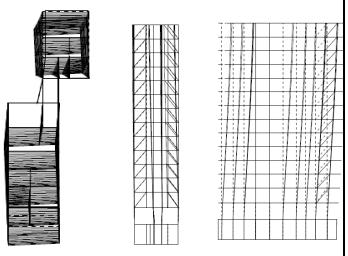	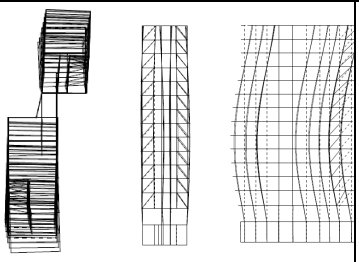	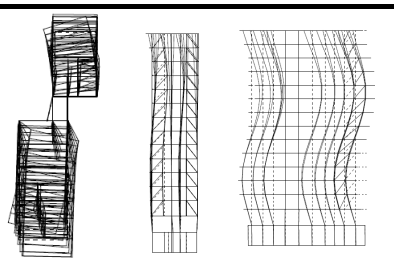
	1.76 [s]	0.53 [s]	0.27 [s]
Rz	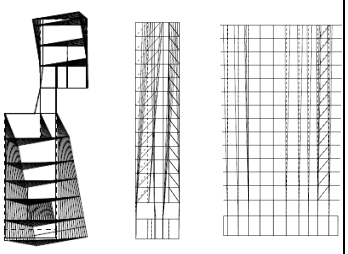	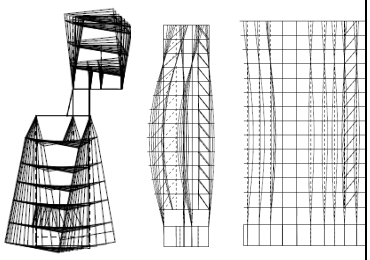	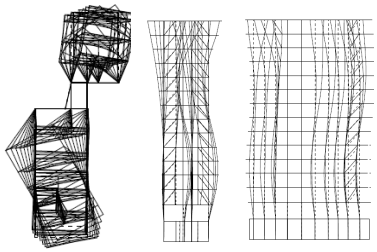
	2.22 [s]	0.63 [s]	0.30 [s]

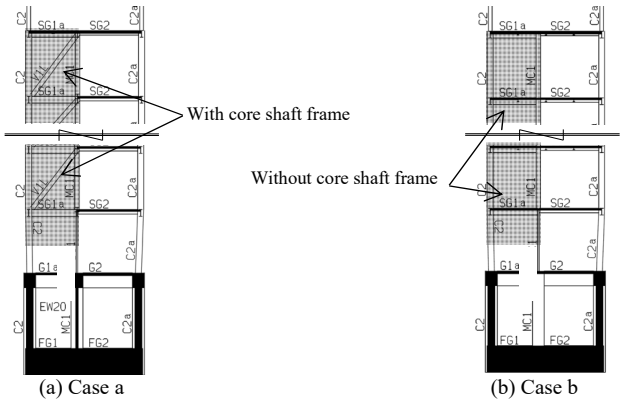

(a) Case a (b) Case b

Fig.3 – Structure with/without core shaft frame

Table 2 – Participation factor of each mode

X direction mode	1st mode		2nd mode	3rd mode
Total mode	1st mode	2nd mode	3rd mode	4th mode
Case a	38.4%	41.6%	19.2%	0.8%
Case b	40.8%	36.5%	14.4%	8.3%
Difference	-2.4%	+5.1%	+4.8%	-7.5%

From the above results, it can be confirmed that the response of the structure in the higher order modes are suppressed by the inclusion of the core shaft frame, and the relative contribution of the first and second modes (that is, equivalent to the X direction first mode) is increased.

3.2 Static characteristics

The vertical distribution of stiffness and eccentricity ratios (as defined in the Japanese Building Code) are shown in Fig. 4(a) and 4(b). In Fig. 4(c), the center of rigidity is plotted in relation to the center of mass at each portion of the building. These figures suggest that there may be significant torsion induced by horizontal forces in the long-side direction (since the distances between the center of mass and stiffness at certain portions is relatively large).

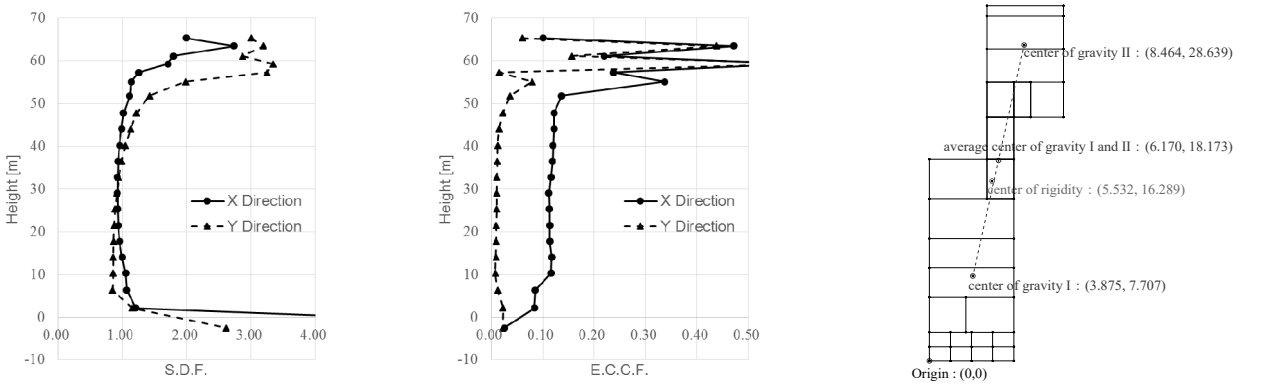

(a) Vertical distribution of stiffness factor

(b) Vertical distribution of eccentricity factor

(c) Positional relationship between centear of gravity and rigidity

Fig.4 – Distribution of rigidity and eccentricity

Fig. 5 and 6 show respectively the story drift and floor rotations of each floor under extremely rare earthquake load. Under that, structures must remain in elastic range by Japanese building code. The story drifts are a range of 1/180 to 1/200 in the short-side direction, and 1/250 to1/350 in the long-side direction. The story rotations due to axial deformation of column caused by axial load fluctuation are in a range of 1/530 to1/550 for most stories, meaning that they contributes about 30% of the total story drifts.

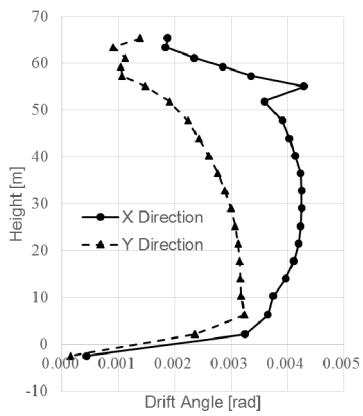

Fig.5 – Vertical distribution of drift angle

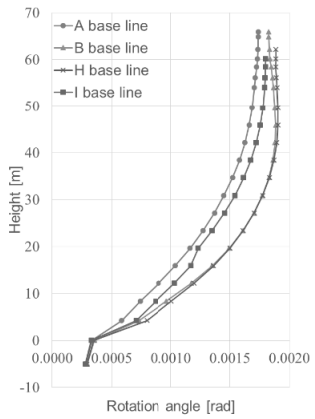

Fig.6 – Rotational angle

As a characteristic of this building, it is designed with the restriction that maximum displacement of top point does not exceed the site boundary (distance 450 mm) on a large-scale earthquake (design ground

motion with a constant velocity response spectrum of 100 cm/s in a long period range) so that the average story drift needs to be suppressed to about 1/145. The plastic ratio is small, and it has been confirmed that the member remains approximately within the elastic limit, although some parts are plasticized.

3.3 Result of vibration measurement

One day after the erection of the structure and installation of interior/exterior walls, cyclic excitation and five-minute long micro-tremor measurements were conducted three times. The cyclic excitation was performed by five people (approx. 65 kg/person x 5) at the center of the gravity in the short-side direction. The variations in applied excitation are presented in Table 3. The spectrum of the measured vibration of the building under Case 2 are plotted in Fig. 7. This clearly shows that the 1st natural frequency of the building is 0.599 Hz and the corresponding period is 1.67 seconds.

Table 3 – Cyclic excitation case (short-side direction)

	Case 1	Case 2	Case 3	Case 4	Case 5	Case 6
Period of vibration (sec)	1.6	1.7	1.8	2.0	2.2	2.4

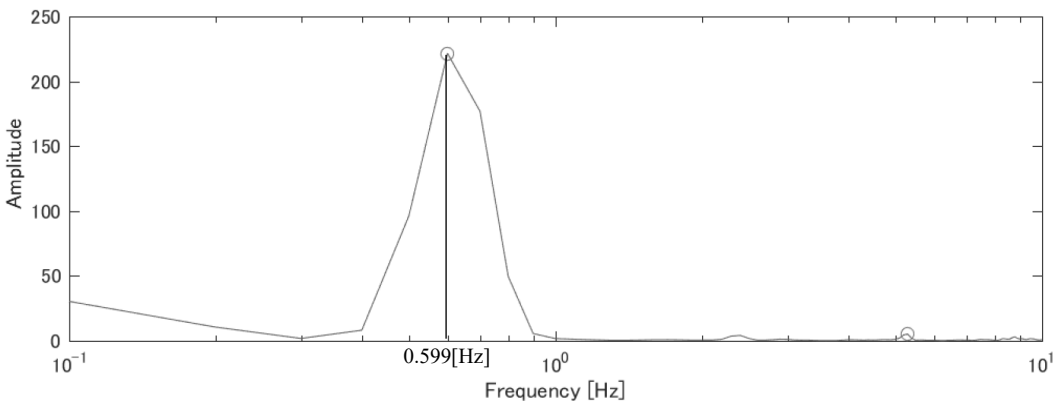

Fig.7 – Power Spectrum of acceleration in short-side direction (Case2)

4. Dynamic Analysis

This section describes the dynamic characteristics of the structure. Dynamic response analysis was performed by applying the ground motions (defined by the velocity response spectrum described in Section 4.1) to the mathematical model described in Section 4.2. Section 4.3 discusses the displacement control effects of the core shaft frames, the viscous dampers and the TMDs.

4.1 Input ground motions

The velocity response spectrum of the applied ground motions is shown in Fig. 8, and the Peak Ground Acceleration (PGA), time step and duration of each wave data are summarized in Table 4. KOKUJI waves are defined in the technical advice notice issued by Japanese authorities in 2016 [6]. They are generated based on actual records of major earthquakes, and they are commonly applied to tall building design in Japan. They share a common property in that the velocity response spectrum for long range periods have a constant value of 100 cm/s. In addition, site waves are generated based on the specific conditions at the site, including the simulated effects of extreme earthquakes, such as the earthquakes in Nankai-Trough in 2016, the South-Kanto region earthquake, and the inland earthquake underneath the Kanto region [2-5]. A KISEISOKU wave is also defined in the technical advice notice issued by Japanese authorities in 2016 [6]. This wave has a peak response in the velocity response spectrum between 5 and 10 seconds, and has a relatively long duration time.

Table 4 – Input ground motion list

Wave name	Detail / Phase	PGA (cm/s^2)	Time step (sec)	Duration (sec)
KOKUJI I	Designed ground motion in legitimate notice (HACHINOHE EW Phase)	507.9	0.02	120.00
KOKUJI II	Designed ground motion in legitimate notice (TOHOKU U. Phase)	481.7	0.02	60.00
KOKUJI III	Designed ground motion in legitimate notice (JMA KOBE NS Phase)	531.6	0.02	60.00
Site I	South-Kanto region earthquake M7.9 (HOKKAIDO RUBESHIBE NS Phase)	447.8	0.01	250.00
Site II	South-Kanto region earthquake M7.9 (HOKKAIDO RIKUBETSU NS Phase)	411.6	0.01	250.00
Site III	South-Kanto region earthquake M7.9 (HOKKAIDO NUKABIRA NS Phase)	406.4	0.01	250.00
Site IV	Nankai Trough earthquake M9.0 Love wave (CHIBA GYOUTOKU NS Phase)	93.9	0.01	327.68
Site V	Nankai Trough earthquake M9.0 Love wave (FUKUSHIMA INAWASHIRO NS Phase)	101.4	0.01	327.68
Site VI	Nankai Trough earthquake M9.0 Love wave (TOKYO TATSUMI NS Phase)	89.4	0.01	327.68
Site VII	Nankai Trough earthquake M9.0 S wave (IBARAKI OMIYA NS Phase)	130.9	0.01	327.68
Site VIII	Nankai Trough earthquake M9.0 S wave (IBARAKI NAKAMINATO NS Phase)	158.3	0.01	327.68
Site IX	Nankai Trough earthquake M9.0 S wave (FUKUSHIMA NAKOSO EW Phase)	160.5	0.01	327.68
Site X	Inland earthquake underneath Kanto region M7.3 (OKAYAMA SHINGO NS Phase)	475.8	0.01	327.68
Site XI	Inland earthquake underneath Kanto region M7.3 (SHIMANE MIHOZEKI NS Phase)	453.6	0.01	327.68
Site XII	Inland earthquake underneath Kanto region M7.3 (TOTTORI AKASAKI NS Phase)	367.3	0.01	327.68
KISEISOKU	KA1 wave (defined in the technical notice)	75.3	0.02	655.36

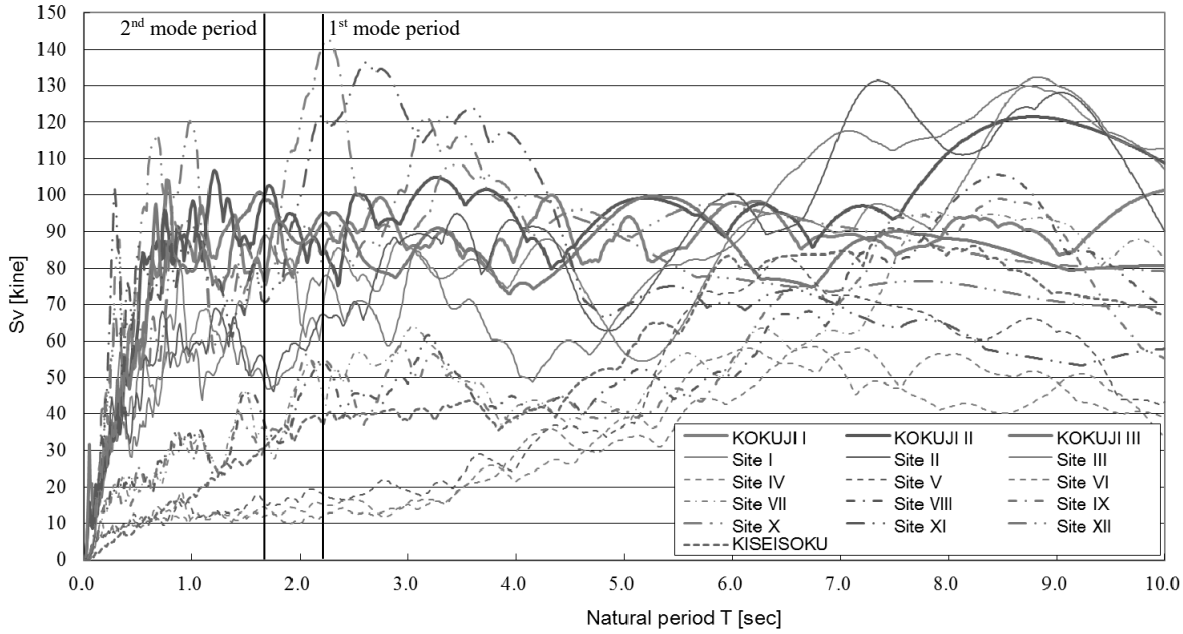

Fig.8 – Velocity response spectrum of input ground motion (h=5%)

4.2 Mathematical analysis model

The concept and detail of the mathematical analysis model is summarised in Fig. 9. The basic ideas are as follows.

1. Using a three-dimensional analysis model (in which the building is modelled to include all structural members), a rigid matrix is developed that is reduced to three degrees of freedom. Rigid floors are represented by a single representative node.
2. The floor diaphragm is considered partially rigid, and non-rigid floors (such as the periphery of the opening and the narrow area) is to evaluate the rigidity of the slab. Also, the 2nd floor is considered non-rigid floor so as to be combined with the inclined column takes into account the axial force that occurs in the girder.
3. The degrees of freedom of TMD nodes are considered only in the X direction.
4. As composite beam effect, φ is set for each member according to the cooperation range of the slab. However, it is assumed that the slab is cracked during a large-scale earthquake and the composite beam effect therefore becomes small (φ=1.0), because of the cyclic deformation of the girder.
5. Vertical springs are used at each pile position, and the influence of rocking due to expansion, contraction, and lifting at the pile is taken into consideration.
6. Consider the rigid area and panel using the member model shown in Fig. 10. The plasticization of the members is taken into account in the MS / MSS placed at the face position.
7. Taking the material non-linearity into consideration, Young's modulus of steel and concrete are taken as follows; E_S=205,000 N/mm^2, $E_C=3.35\times10^4\times(\gamma/24)^2\times(FC/60)^{1/3}$ N/mm^2. The slope of plastic stiffness is 1/100 of elastic stiffness. Here, γ is the air-dry unit weight, FC: design standard strength.
8. The damping effect is 2% of initial stiffness. For viscous dampers and oil dampers, damping is calculated individually.
9. The viscous damper and the oil damper are modelled by springs and dash pots at the member positions. Constitutional rule is respectively Maxwell model and Kelvin-Voigt model, and the hysteresis are shown in Fig. 11.

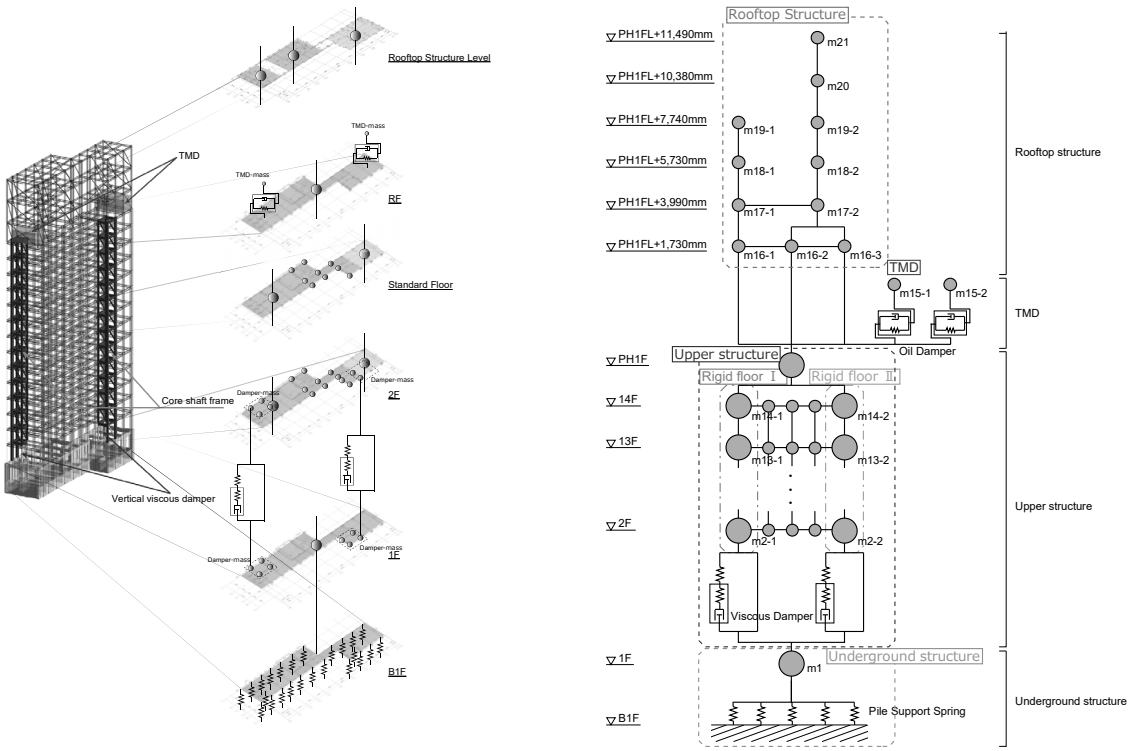

Fig.9 – Mathematical Model

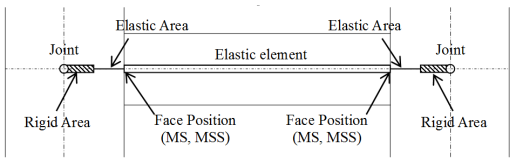

Fig.10 – Element Model

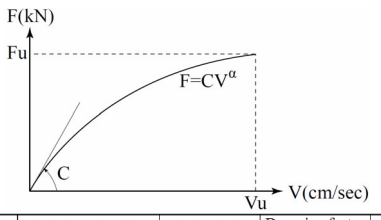

	Limit dampimg force Fu [kN]	Limit velocity Vu [cm/s]	Damping factor C [kN/(cm/s)^α]	α
VD1	2,500	12	1,186	0.3
VD2	2,000	10	1,002	0.3

(a) Vertical viscous damper

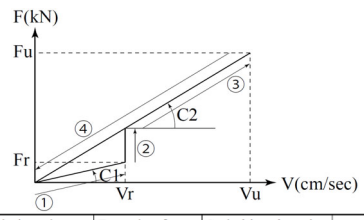

	Limit dampimg force / verocity		Damping factor [kN/(cm/s)]		Switching damping force / velocity		Internal stiffness K [kN/cm]
	Fu [kN]	Vu [cm/s]	C1	C2	Fr [kN]	Vr [cm/s]	
OD1	83.25	185	0.08	0.45	2	25	56

(b) TMD Oil Damper

Fig.11 – Damper Model

4.3 Analysis results

The following three models were analysed and compared for the earthquake motion shown in 3.1.

1. Neither viscous dampers nor oil dampers for TMDs are considered (Model 1)
2. Consider only viscous dampers (Model 2)
3. Consider both viscous dampers and oil dampers for TMDs (Model 3)

The maximum story drift against each ground motion is shown in Fig. 12. In addition, the distribution of story drift for each model and the result of model 1 (damping: 3%, 4% ...) are shown in Fig. 13 for the

notification wave with the largest response (KOKUJI Ⅲ). It can be confirmed that the viscous dampers alone can provide between 2 to 3 % additional damping while the oil dampers in the TMD system can provide between 5 to 14% additional damping, although calculated damping ratios were somewhat different for each input ground motion.

In addition, a sensitivity study was undertaken to assess performance variations in the damping material. The response to the same input ground motion (KOKUJI Ⅲ wave) is compared considering a range of damping ratios between -5 to +10%. The maximum interlayer deformation angle distribution in each case is shown in Fig. 14. From these results, it can be seen that the influence of variation in damping on the response is small. This is explained from the fact that the equivalent attenuation is already reaches about 15%, and the absolute value of the attenuation is sufficiently large. Therefore the influence of fluctuations on the response is relatively low. It is also likely that the response tends to be insensitive as shown in Fig.15 because, as in mid-story isolation systems, the mass ratio of the TMD system is set to about 5% of the 1st mode generalized mass.

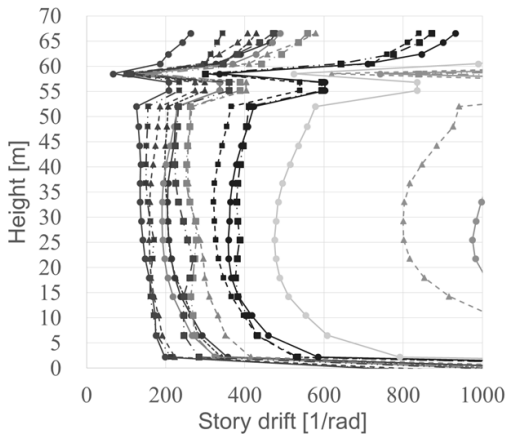

Fig.12 – Maximum story drift against each ground motion

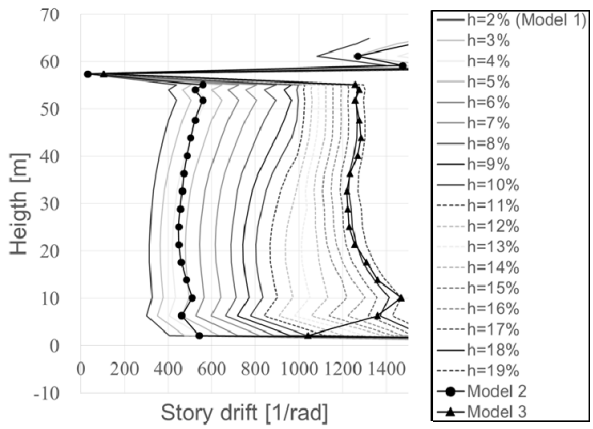

Fig.13 – Maximum story drift of each model (KOKUJI III wave)

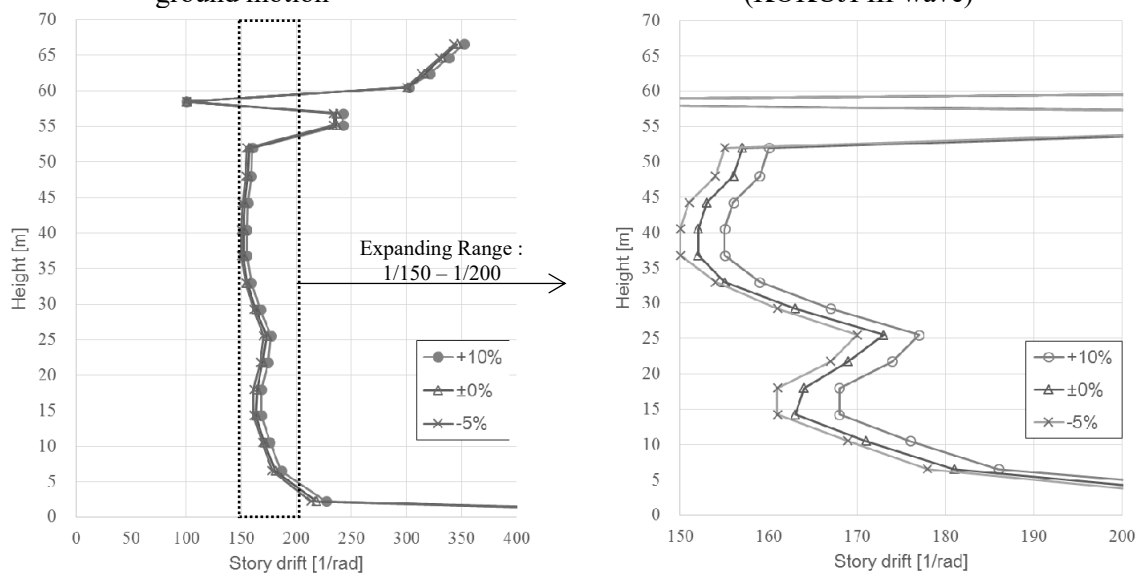

Range : 0 - 1/400

Range : 1/150 – 1/200

Fig.14 – Maximum story drift of model 3 considering variations in damping (KOKUJI III wave)

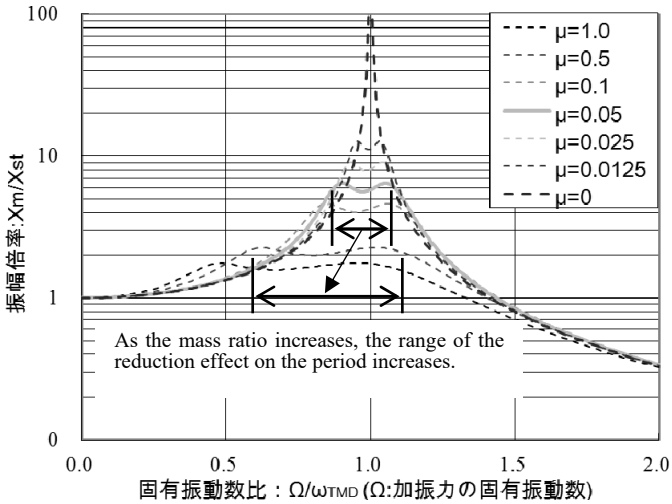

Fig.15 – Optimum damping of TMD dampers and masses

5. Conclusion

This paper has proposed an efficient deformation control system for a super-slender multi-story building by incorporating core shaft frames with vertical viscous dampers at the ground level and TMDs at the roof level into a steel MRF. Through a design example, the paper has also demonstrated that the system can effectively dissipate the dynamic energy using viscous dampers and TMDs, whilst posing no restriction to architectural planning.

Parametric studies have been performed in order to evaluate the impact of different properties of vertical viscous dampers and TMDs on the seismic response of the structure. Three key findings are summarized as follow.

1. Increasing the participation factor of the 1st mode is highly significant for efficiently reducing the horizontal displacement of a super-slender building. It is also clear that damping effects by vertical viscous dampers and TMDs increase if they can be tuned to the mode with a higher participation factor.
2. The viscous dampers alone can provide between 2 and 3% additional damping, whilst the oil dampers in the TMD system can provide between 5 and 14% additional damping. Calculated damping ratios were somewhat different for each input ground motion.
3. The seismic response of this system was found to be insensitive to the properties of the damping devices. This is explained from the fact that buildings with sufficient attenuation have small absolute fluctuations of attenuation even if the damping performance varies somehow. This is also qualitatively explained from the fact that damping mechanisms with heavy mass like TMDs tend to resemble mid-story isolation systems and tend to be less-sensitive [7-10].

It is known that core shaft frames have the effect of greatly improving collapse capacity [11-13]. From the facts shown in this paper, structural design with core shaft frames can improve the structural performance of a slender building (including high-rise buildings) against commonly-assumed design ground motions and even rarer large-scale ground motions.

Refferences

[1] N. Inoue and K. Ikago, “Design of Buildings for Displacement Control,” Maruzen Publishing Co., Ltd., Japan, 2012.

[2] T. Yamane, S. Nagahashi, "A Study on a Generation of Simulated Earthquake Ground Motion Considering Phase Difference Characteristics: Part 4 Generation method of simulated earthquake ground motion with the Fourier amplitude prescribed by the w-square model and the Fourier phase selected based on the standard deviation of the phase difference", Journal of Structural and Construction Engineering, AIJ, Vol.590, p.45-53. 2005.4.

[3] T. Yamane, S. Nagahashi, "A Study on a Generation of Simulated Earthquake Ground Motion Considering Phase Difference Characteristics: Part 6 Generation method of simulated earthquake ground motion in terms of Love waves", Journal of Structural and Construction Engineering, AIJ, Vol.622, p.73-82. 2007.12.

[4] Wald, D. J. and P. G. Somerville : Variable-slip rupture model of the great 1923 Kanto , Japan , earthquake : Geodetic and body-waveform analysis , Bull. Seism. Soc. Am. , 85 , pp.159-177, 1995.2.

[5] Central Disaster Prevention Conference, "Special Committee on Tonankai and Nankai Earthquake, etc.", The 12th and 16th Documents, 2003.12.

[6] Ministry of Land, Infrastructure, Transport and Tourism Housing Bureau Building Guidance Division, "Countermeasures against long-period ground motion caused by huge earthquakes along Nankai Trough in high-rise buildings etc. (technical advice)", No. 1111, 2016.6.

[7] K. Murakami, M. Ishii, K. Miyazaki, and Y. Tsuneki, "Proposal for an Efficient Damping System for High-Rise Buildings in Major Earthquakes", Journal of Disaster Research Vol.10 No.3, 2015.

[8] H. Kida, K. Ikago, and N. Inoue, "Applicability of Force-Restricted Tuned Viscous Mass Dampers to High-Rise Buildings Subjected to Long-Period Ground Motions," 15th World Conference on Earthquake Engineering, Lisbon, Portugal, Paper ID 0138, 2014.

[9] M. Ishii, H. Kazama, K. Miyazaki, and K. Murakami, "Application of Tuned Viscous Mass Damper to Super-High-Rise Buildings," 6th World Conference of the International Association for Structural Control and Monitoring (6WCSCM), Barcelona, Spain, 2014.

[10] K. Miyazaki, M. Ishii, H. Kazama, and K. Murakami, "Robustness of Tuned Viscous Mass Damper Seismic Control system Considering Variation of the Damper Properties," 2013 Summaries of Technical Papers of Annual Meeting, Architectural Institute of Japan, Hokkaido, Japan, Structure-2, pp. 985-986. 2013.

[11] Y. Araki, M. Ohno, R. Kohta, and R. Oka, "Controlling Collapse Mechanism of Tall Steel Frames and Reducing Response to Near-Fault Ground Motions by Base-Hinged Core Trusses," Steel Construction Engineering, Vol.23 No.91, 2016.

[12] B. Alavi, H. Krawinkler, "Strengthening of moment-resisting frame structures against near-fault ground motion effects", Earthquake Engineering and Structural Dynamics, Vol.33, pp.707-722, 2004.

[13] T. Takeuchi, X. Chen, R. Matui, "Seismic performance of controlled spine frames with energy-dissipating member", Journal of Constructional Steel Research, Vol. 114, pp.51-65, 2015.7.

